

Nuclear Localization of Bacterial *Streptoalloteichus hindustanus* Bleomycin Resistance Protein in Mammalian Cells

THIERRY P. G. CALMELS, JEHANGIR S. MISTRY, SIMON C. WATKINS, PAUL D. ROBBINS, ROBIN McGUIRE, and JOHN S. LAZO

Department of Pharmacology (T.P.G.C., J.S.M., R.M., J.S.L.), Department of Cell Biology and Physiology (S.C.W.), and Department of Molecular Genetics and Biochemistry (P.D.R.), University of Pittsburgh School of Medicine, Pittsburgh, Pennsylvania 15261

Received May 19, 1993; Accepted September 2, 1993

Downloaded from molpharm.aspetjournals.org at Thammasat University on December 3, 2012

SUMMARY

Prokaryotes produce a variety of toxins that affect genomic function of both eukaryotes and prokaryotes. The 375-base pair bacterial gene *Streptoalloteichus hindustanus* (Sh) *ble* encodes a small protein, *Streptoalloteichus hindustanus* bleomycin resistance protein (BRP), that inhibits *in vitro* DNA cleavage by the prokaryotic glycopeptide bleomycin, which is a clinically used anticancer drug. NIH/3T3 cells infected with a retroviral vector containing Sh *ble* (SH-9 cells) were highly resistant to the cytotoxicity of bleomycin-like drugs but not to the cytotoxicity of

other, structurally unrelated, DNA-cleaving agents. Expression of BRP did not markedly alter total cellular content or distribution of bleomycin-like compounds. Fluorescently labeled bleomycin was primarily localized in cytoplasmic vesicles in NIH/3T3 and SH-9 cells, whereas BRP, which has no established nuclear localization sequence, was segregated to the nucleus and more specifically to euchromatin. This karyophilic BRP may intercept bleomycin in the nucleus.

BLMs are cationic glycopeptide toxins secreted by prokaryotes that cause sequence-specific DNA single- and double-strand breaks (1, 2). Because these BLMs are also cytotoxic to malignant cells, they are frequently used to treat human malignancies. Recently it has been reported that some aminoglycoside-resistant Gram-negative and Gram-positive bacteria contain genes that confer resistance to BLM. Several of these genes have been identified and sequenced, and all encode small, highly homologous proteins. Examples are genes isolated from the transposon Tn5 (3), from the staphylococcal plasmid pUB110 (4), and from the chromosomal DNA of TLM-producing actinomycetes (the Sh *ble* gene used in this study) (5). There are no known mammalian homologues of these genes or their protein products. The Sh *ble* gene encodes a 14-kDa acidic protein, which reportedly protects against BLM-induced DNA damage *in vitro*, possibly mediated by the ability of the protein to bind to BLM (6). The protein product of the Sh *ble* gene, BRP, has been shown to bind to Fe(II)-BLM with 1:1 stoichiometry (6). In addition, it has been suggested that at least one of these BRPs improves the "fitness" of *Escherichia coli* and may be involved in DNA repair processes (7). The Sh *ble* gene has been expressed in Chinese hamster ovary cells (8) and the recipient cells become resistant to BLM. Surprisingly, there is

no information about the subcellular distribution or functionality of this class of dominant selectable marker gene products in mammalian cells or about the spectrum of cytotoxic agents affected. Thus, we expressed the Sh *ble* gene in NIH/3T3 cells and examined the sensitivity of these infected cells to different BLM analogues and other cytotoxic agents. Furthermore, we studied the subcellular localization of BRP as well as a highly fluorescent BLM analogue.

Materials and Methods

Vectors and virus-producing cells. The replication-defective MFG vector was derived from the Moloney murine leukemia virus, with deleted polymerase (*pol*), envelope (*env*), and *gag* (partial) gene sequences (9). The *gag* gene sequences up to base 1035 were used to increase the packaging efficiency of the unspliced transcript. Viral donor and acceptor sites were used for mRNA splicing. The *Ncol-BgIII* 0.4-kilobase DNA fragment carrying the Sh *ble* gene (5) was inserted into the MFG retrovirus vector digested with *Ncol-BamHI*, to generate the MFG-Sh recombinant vector. The inserted Sh *ble* gene was transcribed from the promoter-enhancer sequence in the retroviral long terminal repeat, and the start codon of the Sh *ble* gene was at the start codon of the deleted *env* gene, at a *NcoI* site. The NIH/3T3-derived ψ-CRIP packaging cell line was kindly provided by Dr. R. Mulligan (Whitehead Institute, Cambridge, MA) (10); NIH/3T3 cells were obtained from the American Type Culture Collection (Rockville, MD) and were maintained in Dulbecco's Vgt-modified Eagle's medium (GIBCO Laboratories, Grand Island, NY) supplemented with 4.5 g/

This work was supported by American Cancer Society Grant DHP77 and National Institutes of Health Grants CA43917 and CA59371.

ABBREVIATIONS: BLM, bleomycin; FLM, fluoromycin; LBM, liblomycin; Sh, *Streptoalloteichus hindustanus*; BRP, *Streptoalloteichus hindustanus* bleomycin resistance protein; TLM, talisomycin; PBS, phosphate-buffered saline; HEPES, 4-(2-hydroxyethyl)-1-piperazineethanesulfonic acid.

liter glucose, 3.7 g/liter NaHCO₃, 10% heat-inactivated fetal bovine serum, 100 units/ml penicillin/streptomycin, and 0.5% HEPES. The Sh *ble* gene was transfected into the amphotropic packaging cell line ψ-CRIP by using the Ca₃(PO₄)₂ co-precipitation method (11). Clones were selected for resistance to BLM (100 μg/ml) and pooled. The culture medium of this ψ-CRIP pool of clones was used as a virus source and was titrated on NIH/3T3 cells. After a 2-hr incubation at 37° in the presence of 8 μg/ml polybrene, medium containing the virus was replaced with fresh medium containing BLM; 48 hr later cells were subcultured. The viral titer was >10⁶ viral particles/ml.

Immunoblotting. Exponentially growing wild-type and Sh *ble*-infected NIH/3T3 cells were harvested and resuspended in 500 ml of 10 mM Tris·HCl buffer, pH 7.5, containing 10 μg/ml leupeptin and 1 mM phenylmethylsulfonyl fluoride. The cells were then lysed by three freeze/thaw cycles, followed by five cycles of sonication (5 sec on ice). After centrifugation for 15 min at 4° at 12,000 × g, the supernatant fraction was isolated and protein content was determined by the method of Bradford (12). A total of 50 μg of protein in a solution containing 50 μM Tris·HCl, pH 6.8, 100 μM dithiothreitol, 2% sodium dodecyl sulfate, 10% glycerol, and 0.1% bromphenol blue were boiled for 5 min, cooled on ice, loaded on a 15% polyacrylamide gel, and then subjected to electrophoresis (4 hr, 200 V). The separated proteins were transferred to a 0.2-μm nitrocellulose membrane and a Western blot was performed as described previously (13). Anti-BRP polyclonal rabbit antiserum or preimmune serum was used at a 1/750 dilution.

Immunocytochemical localization of BRP. Approximately 4 × 10⁴ cells/chamber were plated on a multichamber glass slide (Nunc Inc., Naperville, IL) and incubated for 24 hr at 37°. The immunocytochemistry experiments were achieved as described previously (13). Primary labeling was with anti-BRP rabbit antiserum, preimmune antiserum (approximately 5 μg/ml specific IgG concentration), or irrelevant antiserum. In some experiments the primary antiserum was omitted. For blocking experiments, the anti-BRP rabbit antiserum was coincubated with a 10-fold molar excess of purified BRP before exposure of cells (14).

For "high resolution" fluorescence microscopy and immunoelectron microscopy, the previously published procedures of Khurana *et al.* (15) were followed. The sections were incubated for 30 min in the presence or absence of the primary anti-BRP antibody. No signal was seen in the absence of the primary anti-BRP antibody. In other experiments an antiguicocerebrosidase antibody was used as a control, because the cytoplasmic protein glucocerebrosidase is concentrated in endosomes.

Chemicals. TLM S₁₀₀, TLM A, esperamicin, and clinically used Blenoxane, which is a mixture of BLMs, were supplied by Bristol Myers Squibb (Wallingford, CT). BLM A₂ was isolated from Blenoxane by our previously described fast protein liquid chromatography method (16). FLM was prepared according to the procedure published by Mistry *et al.* (17). LBM was a gift from Nippon Kayaku Co., Ltd. (Tokyo, Japan). Calicheamicin was kindly provided by Dr. L. Hinman (Lederle Laboratories, Pearl River, NY); G418 (geneticin), normal goat serum, goat anti-rabbit peroxidase-conjugated antibody, and streptonigrin were obtained from Sigma Chemical Co. (St. Louis, MO). Neocarcinostatin was obtained from the National Cancer Institute. All chemicals and solvents were from either Fisher Scientific Co. (Pittsburgh, PA) or Aldrich Chemical Co. (Madison, WI). Rabbit anti-BRP antiserum was prepared according to the method described by Perez *et al.* (18).

Cytotoxicity and cell-drug association assays. Exponentially growing wild-type or MFG-Sh-infected NIH/3T3 cells were harvested and centrifuged at 4° for 5 min at 500 × g. Approximately 2000 cells were plated in triplicate into 100-mm culture dishes, and after 5 hr various concentrations of drugs were added. After 6 days at 37° cell survival was determined by clonal assay. The medium was decanted and the cells were gently washed with Ca²⁺/Mg²⁺-free PBS (GIBCO). After the fixing/staining solution (0.25% crystal violet, 10% methanol, 10% formalin, in PBS) was added, the cells were incubated at room temperature for 30 min, washed with distilled water, dried, and assayed for colonies. The colony-forming efficiency for untreated NIH/3T3

cells was between 10% and 20%. Cellular association of FLM or radiolabeled BLM A₂ was determined as described previously (19).

DNA cleavage assays. Supercoiled Bluescript BSKS(+) plasmid DNA (Stratagene, La Jolla, CA) was purified through two sequential CsCl gradients (20) and stored as a stock solution at 4°, in 10 mM Tris·HCl, pH 8, 1 mM EDTA. Immediately before use, the stock DNA solution was diluted 5-fold with 10 mM Tris·HCl, pH 8, to decrease the concentration of EDTA. The appropriate concentration of drug to generate linear or single nicked DNA was calculated and found to be 0.25 μM for BLM A₂, 0.25 μM for TLM S₁₀₀, and 2 μM for FLM. The BRP and different BLM derivatives were added to the reaction mixture containing 0.5 μg of plasmid DNA in 40 mM Tris·HCl, pH 7.5. After 5 min at 25°, the mixture was supplemented with dithiothreitol (2.5 mM) and Fe(NH₄)₂(SO₄)₂ (10 μM) from a freshly prepared solution. DNA integrity was determined by our previously described method (21).

Confocal microscopy. Cells (5 × 10⁴) were plated and allowed to grow on a sterile glass coverslip for 24 hr. Cells were then incubated with 100 μM FLM for 0.15, 1, 5, or 24 hr at 37°. After incubation, cells were washed with PBS, fixed with 2% paraformaldehyde, and viewed under a Zeiss confocal microscope.

Results

Transfer and expression of the Sh *ble* gene. Transfer and expression of the Sh *ble* gene into NIH/3T3 cells were achieved using the recombinant MFG-Sh retrovirus, with a titer of infection of >10⁶ cells. Approximately 100 BLM-selected colonies were pooled, expanded, and selected to generate a population of NIH/3T3 cells highly resistant to BLM, i.e., SH-9 cells. To examine the durability of Sh *ble* expression, we cultured cells for 1 month without BLM and measured BRP levels by Western blot (Fig. 1). A single band equivalent to BRP (14 kDa) was clearly seen in the infected cell line SH-9, and it was absent in the noninfected control NIH/3T3 cells. This demonstrated not only the specificity of the antibody but also the significant production of recombinant BRP by SH-9 cells, which we estimated to be 0.05% of total cell proteins by comparison with the BRP standard protein on Western blot.

Immunocytochemical localization of BRP. The cellular

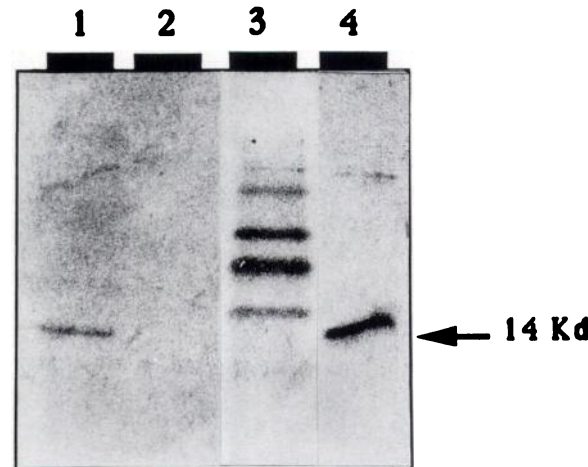


Fig. 1. Immunoblot of NIH/3T3 and SH-9 cells. NIH/3T3 and SH-9 cells (1 × 10⁷) were harvested and lysed, and total protein concentration was determined. Protein (50 μg) from each cell line was loaded on a 15% polyacrylamide gel. After electrophoresis, proteins were transferred to a nitrocellulose membrane and incubated with the anti-BRP polyclonal rabbit antiserum. The BRP band was identified using diaminobenzidine and the secondary anti-rabbit antibody conjugated with peroxidase. Lanes 1 and 2, lysate from SH-9 and NIH/3T3 cells, respectively; lane 3, molecular weight markers; lane 4, pure BRP (150 ng).

distribution of BRP may give significant clues concerning its protective mechanism within eukaryotic cells. When SH-9 cells were permeabilized, incubated with the anti-BRP antibody, and exposed to tetramethylrhodamine isothiocyanate-conjugated goat anti-rabbit secondary antibody, a clearly defined, strong signal was apparent within the cell nucleus (Fig. 2A). NIH/3T3 cells infected with another MFG retrovirus did not exhibit this pronounced nuclear staining, indicating that antibody reactivity was not simply a product of retroviral infection. No label was seen in control NIH/3T3 cells incubated in the same fashion (Fig. 2B) or in SH-9 cells incubated with preimmune antiserum or incubated in the absence of the primary antiserum. Specificity of the anti-BRP antibody was confirmed further by preincubating the anti-BRP antibody with BRP (10-fold molar excess); no labeling for BRP was detected (Fig. 2C). The subcellular localization of BRP was examined further using semi-thin (200-nm) sections of cells. As previously seen with intact cells, semi-thin sections revealed a defined nuclear compartmentalization of the BRP. A striking finding, however, was a complete absence of label within the cellular nucleolus (Fig. 2D), with almost all label appearing to concentrate with a pattern similar to that of nuclear euchromatin.

To investigate further the association of the BRP with DNA, we conducted fine structural studies using immunoelectron microscopy. High resolution electron microscopic studies of the distribution of BRP within SH-9 cells were made by labeling thin (70-nm) sections of cells with antibodies complexed with monodisperse gold particles, affording a resolution of about 9 nm. Again, labeling was abundant within the nucleus in close apposition to morphologically characterized euchromatin and was largely absent from the nucleolus (Fig. 3A) using the immunogold conjugates, which have been characterized to be

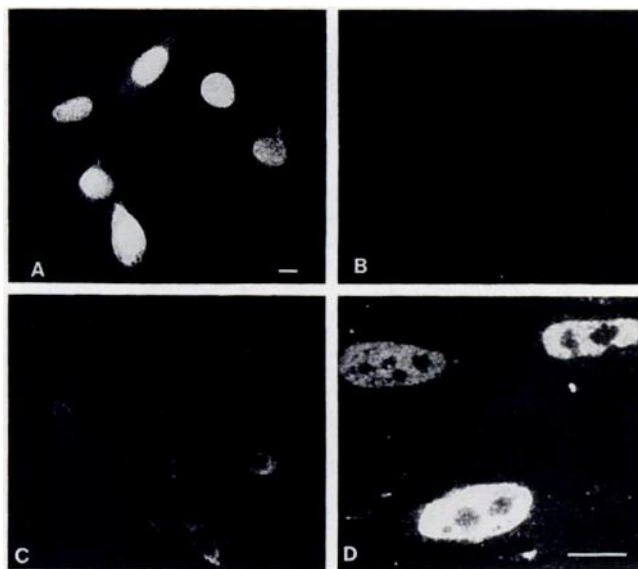


Fig. 2. Immunocytochemical localization of BRP. Exponentially growing NIH/3T3 and SH-9 cells were fixed with paraformaldehyde and permeabilized with Triton X-100. Nonspecific antibody binding was blocked with bovine serum albumin/glycine/goat serum solution and the cells were incubated with anti-BRP rabbit antiserum or preimmune serum. The immunofluorescence was visualized with goat anti-rabbit tetramethylrhodamine isothiocyanate-conjugated secondary antibody. A, SH-9 cells; B, NIH/3T3 cells; C, SH-9 cells treated with anti-BRP rabbit serum that had been previously incubated with excess purified BRP; D, high resolution fluorescence micrograph of SH-9 cells (scale bar = 5 μ m).

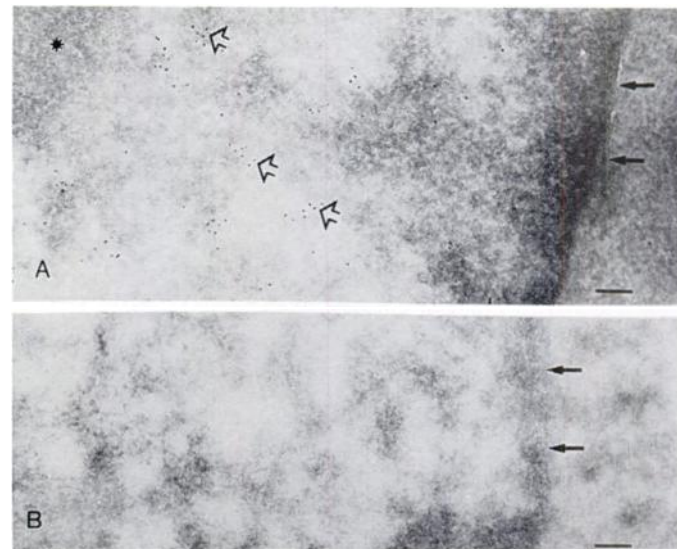


Fig. 3. Immunoelectron micrographs of NIH/3T3 and SH-9 cells. Exponentially growing cells were fixed, scraped, and cut into 1-mm³ cubes after cryoprotection. Cell blocks were then shock frozen and stored in liquid nitrogen. Thin sections were cut and mounted on grids. Nonspecific binding was blocked by incubation of the sections with purified goat IgG. The sections were then incubated with primary anti-BRP antibody and labeled with a 5-nm gold-conjugated goat anti-rabbit antibody. Samples were examined with a Jeol 100cx electron microscope. A, Electron micrograph of SH-9 cells; B, electron micrograph of NIH/3T3 cells. Closed arrows, nuclear membrane; open arrows, BRP localization. *, Nucleolus. (Scale bar = 0.1 μ m).

monodisperse (data not shown). Some label could be detected within the cytoplasm, although significantly less than that seen within the nucleus. This might reflect newly synthesized BRP. The pattern of BRP distribution was markedly different from that seen for glucocerebrosidase, which was found in endosomes and not in the nucleus (data not shown). The nuclear compartmentalization of the BRP was surprising, given that the protein, derived from an anucleate prokaryote, has no known eukaryotic nuclear localization signal (22, 23).

BRP and BLM resistance. Because of the nuclear localization of BRP in NIH/3T3 cells and the putative DNA repair function of the BRP homologue *ble*-Tn5 protein (7), we examined the sensitivity of the wild-type NIH/3T3 and SH-9 cells to DNA-damaging agents including several BLM-like compounds, streptonigrin, X-irradiation, and the enediynes calicheamicin and esperamicin. A representative survival curve for BLM A₂ and IC₅₀ values for a variety of antitumor agents are shown in Fig. 4 and Table 1, respectively. Fig. 4A shows representative survival curves for NIH/3T3 and SH-9 cells with BLM A₂. A concentration of 3 μ M BLM A₂ killed 99% of the NIH/3T3 cells, whereas SH-9 cells remained resistant. We estimated a minimum of 10,000-fold BLM A₂ resistance for SH-9 cells, relative to NIH/3T3 cells. This is, to our knowledge, the highest BLM resistance level ever observed in mammalian cells, indicating the efficacy of BRP. NIH/3T3 cells infected with a MFG-*lacZ* retrovirus, and expressing only the *lacZ* gene, exhibited the same BLM sensitivity as did wild-type NIH/3T3 cells. Table 1 summarizes results examining the relationship between the expression of the Sh *ble* gene and resistance to a variety of BLM analogues as well as other DNA-damaging agents. Interestingly, the magnitude of resistance to BLM-like drugs differed. The IC₅₀ of infected SH-9 cells was approxi-

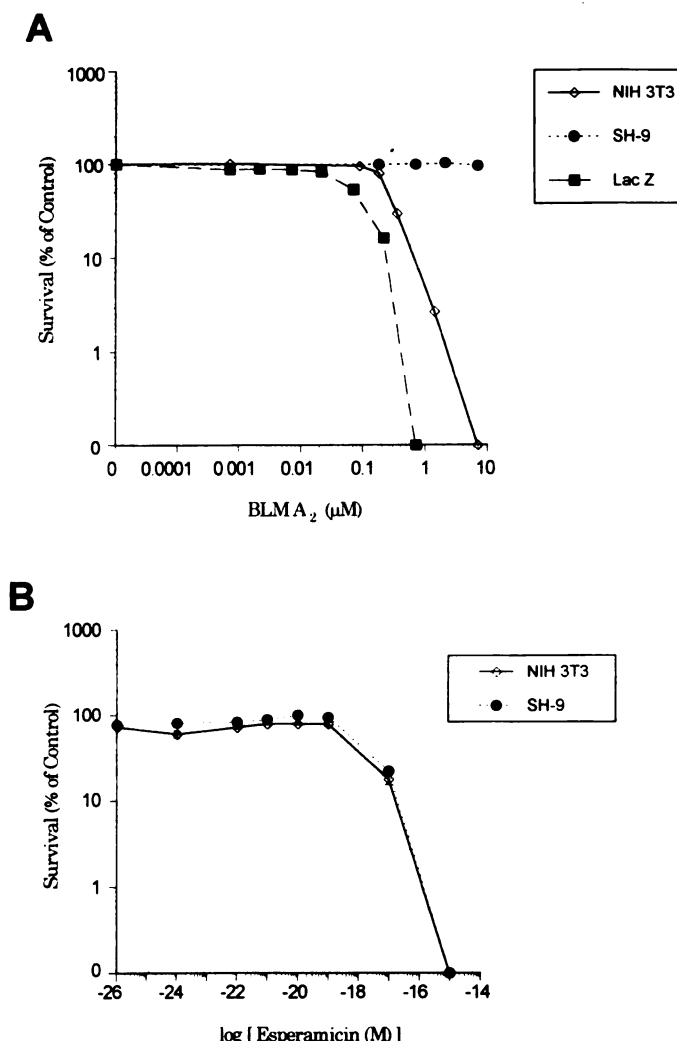


Fig. 4. Concentration-response curves for NIH/3T3 and SH-9 cells with continuous BLM A₂ (A) or esperamicin (B) exposure. Approximately 2000 cells were plated in 100-mm culture dishes and various concentrations of BLM A₂ or esperamicin were added. Cells were incubated at 37° for 6 days and cell survival was determined by clonal assay.

TABLE 1

Drug sensitivities of NIH/3T3 and SH-9 cells

Cells were exposed to drugs for 6 days and inhibition of cellular growth was determined using a clonal assay as described in Materials and Methods. Untreated NIH/3T3 and SH-9 cells had approximately 500 colonies/plate. The resistance index is indicated in parentheses and was calculated as the IC₅₀ of SH-9 cells divided by the IC₅₀ of the parental line.

Compound	IC ₅₀	
	NIH/3T3	SH-9
BLM A ₂	0.02 μM	210 μM (10 ⁴)
TLM S _{10b}	0.5 μM	6.0 μM (12)
FLM	5.2 μM	52 μM (10)
TLM A	0.35 μM	17.5 μM (50)
LBM	0.25 μM	5.0 μM (20)
Geneticin	0.1 μM	0.1 μM
Streptonigrin	1.0 nM	1.0 nM
Calicheamicin	0.1 nM	0.1 nM
Esperamicin	1.0 pM	1.0 pM

mately 10-fold higher for TLM S_{10b} and FLM, compared with the wild-type cells. Cells producing BRP showed intermediate levels of resistance to TLM A (50-fold) and LBM (20-fold), compared with uninfected NIH/3T3 cells. In contrast, no difference was observed between the two cell lines exposed to the other DNA-damaging agents. Fig. 4B shows representative survival curves for NIH/3T3 and SH-9 cells exposed to various concentrations of esperamicin and illustrates the lack of resistance in the SH-9 cells. Streptonigrin, which like BLM cleaves purified DNA and requires a reducing agent and a metal to be activated, was equally toxic to infected and uninfected NIH/3T3 cells. Similar results were seen with X-irradiation. Thus, the BRP-derived resistance appears to be specific to the BLM-like compounds and is consistent with the hypothesis that protection results from selective protein binding to the BLM.

BRP and DNA damage. We next studied the effect of coincubation of BRP with three BLM analogues on the ability of these analogues to cleave DNA. Fig. 5 shows the gel electro-

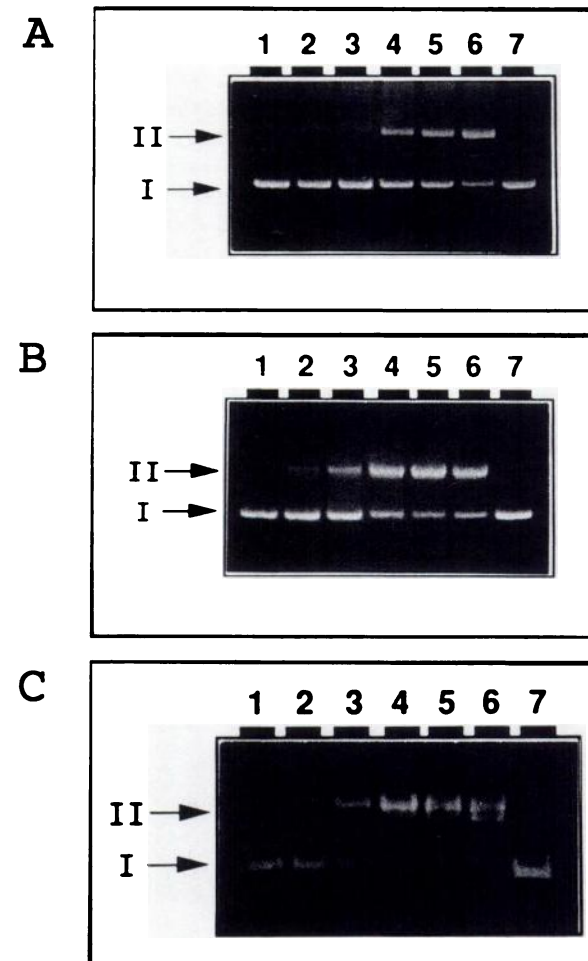


Fig. 5. Protection from BLM A₂, TLM S_{10b}, and FLM-induced DNA cleavage by BRP. Bluescript BSKS(+) plasmid DNA was incubated at 4° for 20 min with BLM A₂ (0.25 μM) (A), TLM S_{10b} (0.25 μM) (B), or FLM (2.0 μM) (C), in the presence or absence of various concentrations of BRP. The loss of covalently closed, circular (form I) DNA and the appearance of single nicked (form II) and linear (form III) DNA were determined by agarose gel electrophoresis. Lanes 1 and 7, plasmid DNA incubated without and with Fe(II), respectively (no drug or protein); lanes 2-5, plasmid DNA incubated with a Fe(II)-bound drug to BRP molar ratio of 1:10, 1:5, 1:1, and 1:0.5, respectively; lane 6, plasmid DNA incubated with the Fe(II)-bound drug alone.

phoretic patterns of DNA integrity after exposure to three BLM analogues in the absence or presence of BRP. Because the analogues exhibited different activity levels and potencies, the appropriate concentrations necessary to generate single nicked DNA from covalently closed, circular plasmid DNA were individually determined (see Materials and Methods). The potency of FLM was approximately 8-fold lower than that of TLM S_{10b}, which was used as a precursor to synthesize FLM. This reduction in potency for LBM and FLM was expected, due to the modification of the carboxyl-terminal amine region of the core glycopeptide (24). A 10-fold excess concentration of BRP was able to protect the plasmid DNA against cleavage by all the BLM-like compounds tested. No protection against plasmid DNA damage produced by esperamicin or streptonigrin was seen with BRP.

Drug content and subcellular localization. Because genomic DNA is thought to be the principal target of BLM (1) and BRP colocalized with the nuclear chromatin, we analyzed the cellular content of BLM and FLM and the subcellular distribution of FLM (a fluorescent BLM mimic) in Sh *ble*-expressing SH-9 cells. When NIH/3T3 wild-type and SH-9 cells were incubated with 1 μ M [³H]BLM A₂ for 1 hr, we could detect no significant difference in cellular drug accumulation. The NIH/3T3 wild-type and SH-9 cells had approximately 4 pmol of [³H]BLM A₂/10⁷ cells (Table 2). FLM, which is fluorescein-labeled TLM S_{10b}, was also used to examine drug uptake, as well as subcellular distribution in SH-9 cells. Consistent with our results using [³H]BLM A₂, we found no significant difference in the cellular fluorescence between uninfected and retrovirus-infected cells (approximately 50 pmol/10⁷ cells) after a 1-hr incubation with 100 μ M FLM (Table 2). Thus, expression of the Sh *ble* gene does not appear to alter the total drug content of either BLM A₂ or FLM. The karyophilic protein BRP also did not alter the apparent distribution of FLM, compared with that seen in NIH/3T3 cells (Fig. 6). In uninfected and retrovirus Sh *ble*-infected NIH/3T3 cells, FLM was observed throughout the cytoplasm after a 10-min incubation, whereas after 1 or 5 hr the fluorescent compound was concentrated in the perinuclear area (data not shown). No detectable fluorescence was seen in the nucleus, at least in the first hour of incubation. After 5 hr of FLM exposure, a few weak fluorescent foci were seen in the nucleus.

Discussion

Most nuclear proteins are concentrated in the nucleus by a specific, energy-dependent, transport process (22). The existence of nuclear transport signals has been firmly established, and many nuclear localization sequences consisting of approx-

TABLE 2

Cellular association of BLM A₂ and FLM in NIH/3T3 and SH-9 cells

Exponentially growing cells (1 \times 10⁶) were incubated in suspension with either 1 μ M [³H]BLM A₂ or 100 μ M FLM for 1 hr at 37°. Cells were washed with ice-cold PBS and cell-associated radioactivity or fluorescence was measured using a scintillation counter or a fluorescence spectrophotometer (excitation, 497 nm; emission, 523 nm), respectively. Each value is the mean \pm standard error of four experiments.

Cells	Cellular association	
	BLM A ₂	FLM
	pmol/10 ⁷ cells	
NIH/3T3	4.1 \pm 0.32	49 \pm 2.4
SH-9	4.9 \pm 0.24	61 \pm 3.2

imately 10 positively charged amino acids have been identified (25). Some proteins that lack a defined nuclear localization sequence enter the nucleus with other proteins acting as co-transporters (26). Microinjection studies have shown that various small proteins lacking the nuclear localization signal can simply diffuse across the nuclear envelope (27). Non-nuclear proteins smaller than approximately 40–60 kDa often equilibrate between the nucleus and the cytoplasm, whereas larger proteins are excluded from the nucleus (27). A key finding of the present study is the karyophilic nature of the bacterial BRP with NIH/3T3 cells. This is interesting because the BRP does not contain any known or putative nuclear localization sequence. The mechanism by which the BRP reaches the nucleus is not known (27). It is thought that the binding of the acidic nucleoplasmin to basic histones is due to charge shielding (28). Because BRP is highly negatively charged at physiological pH, its retention in the chromatin might reflect a charge interaction with positively charged histones or polyamines. The clustered association of BRP with euchromatin is consistent with this notion. Exclusion from the nucleoli may be due in part to the high concentration of negatively charged B23 protein or the higher density of the nucleolus (29). We do not believe that BRP binds directly to DNA, because no shift in BSKS(+) plasmid DNA was seen during electrophoresis (Fig. 5) and we have not seen changes in the gel filtration profile of radiolabeled DNA incubated with BRP (data not shown). The BRP represents the first example known to us of a bacterial protein that is localized in the nucleus of mammalian cells without being artificially engineered by insertion of a nuclear localization sequence (23).

Previous binding studies by Gatignol *et al.* (6) demonstrated both high and low affinity interaction between Fe(II)-BLM and BRP; with 400 nM BRP they found half-saturating concentrations of 55 \pm 10 and 220 \pm 70 nM. BRP was also capable of blocking BLM-mediated DNA damage. We extended these observations and found that BRP blocked DNA damage induced by a variety of BLM analogues. Thus, we conclude that BRP recognizes a large part of the BLM molecule, which was predicted by Gatignol *et al.* (6). The metal binding domain is identical in all of the BLM analogues studied, and this domain may be a major site of BRP interaction. Because BRP does not block toxicity of other DNA-damaging agents, we believe that proteins of this family act as BLM-binding proteins and not, as has been hypothesized by Blot *et al.* (7), as DNA repair proteins.

Because of the BLM-binding property of BRP (6), we compared the cellular accumulation/distribution of BLM and FLM in wild-type and Sh *ble*-containing NIH/3T3 cells. We previously reported (17) that BLM-sensitive and -resistant cells displayed different distributions of FLM. NIH/3T3 cells are naturally resistant to BLM, compared with other cells such as A253 cells, and the cytoplasmic localization was useful in our studies. The expression of the Sh *ble* gene in NIH/3T3 cells does not influence the penetration and the cellular association of BLM and FLM. In addition, the localization of FLM is not altered by BRP production in the infected SH-9 cells. Previous studies (17, 30, 31) indicated that cells do not concentrate BLM. A small fraction of the extracellular drug is found to be associated with the cell and <15% of this localizes in the nucleus (31). In the present study, FLM-associated fluorescence was shown to be localized in the perinuclear area of uninfected

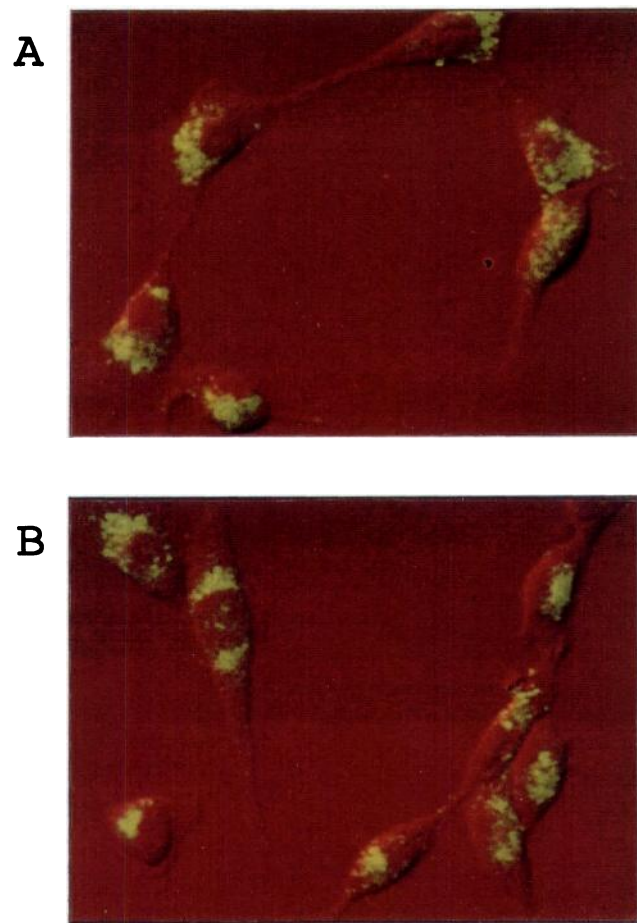


Fig. 6. Confocal micrographs of NIH/3T3 and SH-9 cells incubated with FLM. Cells (5×10^4) were plated on a sterile glass coverslip and allowed to incubate with $100 \mu\text{M}$ FLM for 5 hr at 37° . After incubation cells were fixed with 2% paraformaldehyde and viewed under a Zeiss confocal microscope using a fluorescein filter. A, NIH/3T3 cells; B, SH-9 cells.

or retrovirus Sh *ble*-infected NIH/3T3 cells. The mechanism by which BLM reaches the nucleus is not known and the nuclear envelope could be a key regulatory factor responsible for sensitive or resistant BLM phenotypes. We hypothesize that BLM leaks in small amounts into the nucleus, where BRP might neutralize the drug by binding it, thereby protecting the cell from being damaged.

The clinical use of BLM enhances the significance of our results. Although BLM is used to treat certain forms of cancer, its use has been significantly curtailed by a high incidence of adverse effects such as life-threatening pulmonary fibrosis (32). Pharmacological approaches to limit this pulmonary toxicity of BLM have been generally disappointing. As demonstrated in this study, the BRP is extremely effective in protecting cells against BLM toxicity. Thus, the BRP might be useful in preventing BLM-induced pulmonary toxicity if the small Sh *ble* gene could be expressed exclusively in the lung, making it a potential candidate for gene therapy.

Acknowledgments

We thank Professor Gerard Tiraby (University of Paul Sabatier, Toulouse, France) and CAYLA Company (Toulouse, France) for providing us with the anti-BRP antisera, the Sh *ble* gene, and the purified BRP; Dr. Gunhild Mueller and Lori Nalitz for making the retroviral construct; Dr. Chuck Walsh for assistance with FLM confocal microscopy; and Carl Johnson, Fran Shagas, and Alan Fredrickson for their excellent technical help. We are also grateful for helpful discussions with Drs. Bruce R. Pitt, Said M. Sebti, and Jim Rusnak and members of the Lazo laboratory and for the skilled secretarial assistance of Sharon Webb.

References

- Umezawa, H. Advances in bleomycin studies, in *Bleomycin: Chemical, Biochemical and Biological Aspects* (S. M. Hecht, ed.). Springer-Verlag, New York, 24–36 (1979).
- Lazo, J. S., J. C. Schisselbauer, B. Meandzia, and K. A. Kennedy. Initial single-strand DNA damage and cellular pharmacokinetics of BLM A₂. *Biochem. Pharmacol.* **36**:2207–2213 (1989).
- Mazodier, P., P. Coesart, E. Giraud, and F. Gasser. Completion of the nucleotide sequence of the central region of tn5 confirms the presence of three resistance genes. *Nucleic Acids Res.* **13**:195–205 (1985).
- Simon, D., N. Rao Movva, T. F. Smith, M. El Alama, and J. Davies. Plasmid-determined bleomycin resistance in *Staphylococcus aureus*. *Plasmid* **17**:46–53 (1987).
- Drocourt, D., T. P. G. Calmels, J. P. Reynes, M. Baron, and G. Tiraby. Cassettes of the *Streptococcus hindustanus ble* gene for transformation of lower and higher eukaryotes to phleomycin resistance. *Nucleic Acids Res.* **18**:4009 (1990).
- Gatignol, A., H. Durand, and G. Tiraby. Bleomycin resistance conferred by a drug binding protein. *FEBS Lett.* **230**:171–175 (1988).
- Blot, M., J. Meyer, and W. Arber. Bleomycin resistance gene derived from the transposon Tn5 confers selective advantage to *Escherichia coli* K12. *Proc. Natl. Acad. Sci. USA* **88**:9112–9116 (1991).
- Mulsant, P., A. Gatignol, M. Dalena, and G. Tiraby. Phleomycin resistance as a dominant selectable marker in CHO cells. *Somat. Cell Mol. Genet.* **14**:243–252 (1988).
- Ohashi, T., S. Boggs, P. Robbins, A. Bahnsen, K. Patrene, F. S. Wei, J. F. Wei, J. Li, L. Lucht, Y. Fei, S. Clark, M. Kimak, H. He, P. Mowery-Rushton, and J. A. Barranger. Efficient transfer and sustained high expression of the human glucocerebrosidase gene in mice and their functional macrophages following transplantation of bone marrow transduced by a retroviral vector. *Proc. Natl. Acad. Sci. USA* **89**:11332–11336 (1992).
- Danos, O., and R. C. Mulligan. Safe and efficient generation of recombinant retroviruses with amphotropic and ecotropic host ranges. *Proc. Natl. Acad. Sci. USA* **85**:6460–6464 (1988).
- Chen, C., and H. Okayama. High efficiency transformation of mammalian cells by plasmid DNA. *Mol. Cell. Biol.* **7**:2745–2752 (1987).
- Bradford, M. M. A rapid and sensitive method for the quantitation of microgram quantities of protein utilizing the principle of protein-dye binding. *Anal. Biochem.* **72**:248–254 (1976).
- Byers, T. J., L. M. Kunkel, and S. C. Watkins. The subcellular distribution of dystrophin in mouse skeletal, cardiac, and smooth muscle. *J. Cell Biol.* **115**:411–421 (1991).
- Calmels, T. P. G., F. Martin, H. Durand, and G. Tiraby. Proteolytic events in the processing of secreted proteins in fungi. *J. Biotechnol.* **17**:51–66 (1990).
- Khurana, T. S., S. C. Watkins, and L. M. Kunkel. The subcellular distribution of chromosome 6-encoded dystrophin-related protein in the brain. *J. Cell Biol.* **119**:357–366 (1992).
- Mistry, J. S., S. M. Sebti, and J. S. Lazo. Separation of bleomycins and their deamido metabolites by high-performance cation-exchange chromatography. *J. Chromatogr.* **514**:86–90 (1990).
- Mistry, J. S., J. P. Jani, G. Morris, R. B. Mujumdar, I. J. Reynolds, S. M. Sebti, and J. S. Lazo. Synthesis and evaluation of fluoromycin: a novel fluorescence-labeled derivative of talisomycin S_{1a}. *Cancer Res.* **52**:709–718 (1992).
- Perez, P., G. Tiraby, J. Kallerhoff, and J. Perret. Phleomycin resistance as a dominant selectable marker for plant cell transformation. *Plant Mol. Biol.* **13**:365–373 (1989).
- Morris, G., J. S. Mistry, J. R. Jani, S. M. Sebti, and J. S. Lazo. Cysteine proteinase inhibitors and bleomycin-sensitive and -resistant cells. *Biochem. Pharmacol.* **41**:1559–1566 (1991).
- Sambrook, J., E. F. Fritsch, and T. Maniatis. *Molecular Cloning: A Laboratory Manual*, Ed. 2. Cold Spring Harbor Laboratory, Cold Spring Harbor, NY (1989).
- Lazo, J. S., W. N. Hait, K. A. Kennedy, I. D. Braun, and B. Meandzia. Enhanced bleomycin-induced DNA damage and cytotoxicity with calmodulin antagonists. *Mol. Pharmacol.* **27**:387–393 (1985).
- Hanover, J. A. The nuclear pore: at the crossroads. *FASEB J.* **6**:2288–2295 (1992).
- Silver, P. A. How proteins enter the nucleus. *Cell* **64**:489–497 (1991).
- Wassermann, K., L. A. Zwelling, J. W. Lown, J. A. Hartley, K. Nishikawa, J. Lin, and R. A. Newman. Liblomycin-mediated DNA cleavage in human head and neck squamous carcinoma cells and purified DNA. *Cancer Res.* **50**:1732–1737 (1990).
- Kalderon, D., B. L. Roberts, W. D. Richardson, and A. E. Smith. A short amino acid sequence able to specify nuclear location. *Cell* **39**:499–509 (1984).
- Dingwall, C., and R. Laskey. The nuclear membrane. *Science (Washington D. C.)* **258**:942–947 (1992).
- Peters, R. Fluorescence microphotolysis to measure nucleocytoplasma transport and intracellular mobility. *Biochim. Biophys. Acta* **864**:305–359 (1986).
- Earnshaw, N. C., B. M. Honda, and R. A. Laskey. Assembly of nucleosomes: the reaction involving *X. laevis* nucleoplasm. *Cell* **21**:373–383 (1980).
- Breeuwer, M., and D. S. Goldfarb. Facilitated nuclear transport of histone H1 and other small nucleophilic proteins. *Cell* **60**:999–1008 (1990).
- Roy, S. M., and S. B. Horwitz. Characterization of the association of radio-labeled bleomycin A2 with HeLa cells. *Cancer Res.* **44**:1541–1546 (1984).
- Lazo, J. S., I. D. Braun, D. C. Larabee, J. C. Schisselbauer, B. Meandzia, R. A. Newman, and K. A. Kennedy. Characteristics of bleomycin-resistant phenotypes of human cell sublines and circumvention of bleomycin resistance by liblomycin. *Cancer Res.* **49**:185–190 (1989).
- Lazo, J. S., D. G. Hoyt, S. M. Sebti, and B. R. Pitt. Bleomycin: a pharmacological tool in the study of the pathogenesis of interstitial pulmonary fibrosis. *Pharmacol. Ther.* **47**:347–358 (1990).

Send reprint requests to: John S. Lazo, Department of Pharmacology, E1346 Biomedical Science Tower, University of Pittsburgh, Pittsburgh, PA 15261.